New Panel Method for Supersonic Flows About Arbitrary Configurations

Yuichi Maruyama*
Mitsubishi Electric Corporation, Kanagawa, Japan
Sadao Akishita†
Mitsubishi Electric Corporation, Hyogo, Japan
and
Akihito Nakamura‡
Mitsubishi Space Software Corporation, Kanagawa, Japan

Steady supersonic linearized potential flows about several types of configurations are simulated using a new panel-method program. Linear distribution of doublet is adopted to ensure the continuity of the strength on panel edges, while both constant and linear distributions are examined for source. Morino's scheme is employed in most cases. The velocity boundary condition scheme is also applied in some cases. The results show good agreement with analytical solutions or wind-tunnel tests unless perturbation is too large to justify the linearization. The computation time is within a reasonable limit, and the program size is comparable to that of the panel method for incompressible or subsonic flow.

Nomenclature

a_{ij}, b_{ik}	= influence coefficients
C_D	= drag coefficient
C_{D0}	= zero-lift drag coefficient
C_p	= pressure coefficient
C_L	= lift coefficient
M	= freestream Mach number
u, v, w	= perturbation velocity
x	= axial or chordwise coordinate
α	= angle of attack
δ	= cone half-angle
θ	= semiwedge angle
μ	= doublet strength
σ	= source strength

Subscripts

i	= inner control-point index number
i'	= outer control-point index number
j	= nodal-point index number for doublet
k	= nodal-point index number for source
$j$max, $k$max	= total numbers of nodal points on the body panels

Introduction

TO analyze flight mechanics of aircrafts or missiles, it is necessary to know their aerodynamic characteristics precisely. Among the current methods of computational fluid dynamics, panel methods are considered to be most practical because of the arbitrariness of body shapes and the low cost of computation. Panel methods, which are often used in analyzing incompressible or subsonic flow around arbitrary configurations,[1] are also known to be applicable to supersonic flow. However, there exist additional difficulties, since the fundamental equation is of the hyperbolic type. Great efforts have been devoted to developing panel-method programs for supersonic flow, such as USSAERO[2] and PAN AIR,[3,4] and it was found necessary to implement the following two requirements: 1) continuity of doublet strength and contiguity of panel surface must be ensured on panel edges, and 2) source and doublet must obey Green's formula, i.e., perturbation potential must be zero outside the real-flow region. Here, the first requirement arises from the need for continuity of potential across the downstream characteristic surfaces departing from panel edges. The second requirement is needed to prevent a spurious Mach wave from being propagated into the body, penetrating panels on the opposite side, and then entering the real-flow region again.

In the development of a new panel-method program MARCAP (Mitsubishi's Arbitrary Configuration Aerodynamic Program), the two requirements are considered as the basis of the scheme, but in other aspects, the program is improved radically compared to the conventional ones. Clear distinctions between panels, nodal points, and control points are found to be useful in simplifying the scheme. Triangular panels are used to provide contiguity of surface along panel edges. Linear distribution is adopted for the doublets to satisfy the first requirement, while both constant and linear distributions are examined for the sources, and the results are compared. Morino's boundary condition[5] is employed for simplicity, but the velocity boundary condition (VBC), which strictly ensures flow tangency, is also applied in some cases, and the results are compared. The program is tested for simple configurations such as cones, a two-dimensional double-wedge wing, and a delta wing with a diamond section. Then the results are compared with analytical solutions and also with the results of previous work. Next, flows around wing-body configurations (AGARD-A and -B models) are simulated and compared with wind-tunnel tests.

General Description of the Program

Definition of Nodal Point and Control Point

Constructing the new simplified scheme, a nodal point and a control point are redefined as follows: a nodal point is the point location where the source strength and/or doublet

Presented as Paper 86-2181 at the AIAA Atmospheric Flight Mechanics Conference, Williamsburg, VA, Aug. 18-20, 1986; received Jan. 11, 1987; revision received May 16, 1987.

*Aerodynamic Engineer, Kamakura Works.
†Research Engineer, Central Research Laboratory. Member AIAA.
‡Software Engineer.

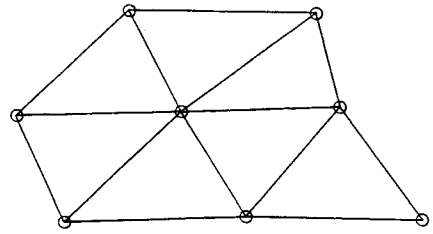

⊙ nodal point
for linear distribution

Fig. 1 Panels and nodal points.

strength is assigned, and a control point is the point location where the potential value or the velocity vector is evaluated. The redefinition of a nodal point makes it easier to determine a higher-order distribution of source and/or doublet in a simple manner. A nodal point and a control point have different roles as stated; therefore, both need not agree with each other.

Definition of Nodal Point

Because of the first requirement, the strength of doublet cannot be constant on each panel, and a higher-order panel method is needed for simulation of a supersonic flow. Consider a singularity such as source or doublet distributed on an assembly of contiguous panels, and that its strength on each panel obeys a polynomial function of coordinates defined on the panel. The distribution of source and/or doublet on the whole panel assembly can be determined by its strength at a finite number of points distributed on the panel assembly in a definite manner. These points may be called "nodal points," for they are often distributed on the nodes of the panel assembly.

A nodal point and a panel play different roles: the former is the point location where the strength of the singularity is assigned, while the latter is a geometrical unit of the discretized shape of the boundary surface. Consequently, the total number of the former need not coincide with that of the latter except for a zeroth order distribution, i.e., a constant strength on each panel. If an unreasonable restriction that both numbers be equal were imposed in a higher-order method, the computational scheme would become irrationally complicated. For example, the PAN AIR scheme adopts linear and quadratic distribution for source and doublet, respectively, but the total number of nodal points and panels are set to be equal. This requires a lot of skillful techniques such as least-squares fits, subdivision of panels, and so on, to determine the distribution of singularities.

MARCAP adopts triangular panels. For linear distribution, nodal points are set on the panel vertices, each of which commonly belongs to its adjacent panels (see Fig. 1). On the other hand, the panels themselves can be regarded as the nodal points for constant distribution. Consequently, the number of unknown parameters determining the distribution on each panel is exactly equal to the number of the nodal points on the panel (including the vertices) for both types of distribution. Continuity of strength is ensured on panel edges for linear distribution, since the distribution on each edge is determined uniquely by the strength on the nodal points at both ends of the edge. Moreover, there is no need for average planes, since triangular panels are always planar, and contiguity of panels is always satisfied.

Definition of Control Point

The Prandtl-Glauert equation for supersonic flow can be transformed into an integral equation as follows:[6]

$$\phi(P)=\frac{1}{2\pi}\int_{S_w}^{*}\mu\frac{\partial}{\partial n_c}\left(\frac{1}{R}\right)\mathrm{d}S-\frac{1}{2\pi}\int_{S_w}\frac{\sigma}{R}\mathrm{d}S \tag{1}$$

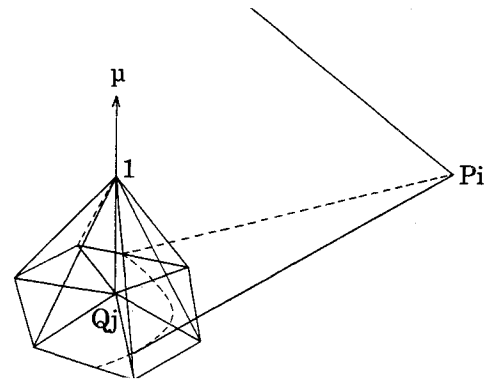

Fig. 2 Illustration of the physical meaning of an influence coefficient for linear distribution.

where ϕ = perturbation velocity potential, R = hyperbolic distance between P and Q, $\partial/\partial n_c$ = spatial derivative to the direction of conormal on dS, S_w = point P's dependence domain part of boundary surface S, $*\int \mathrm{d}S$ = finite part of the integral, and Q = a point on dS. If source and doublet are distributed according to Green's formula to satisfy the second requirement stated earlier, they are defined as follows:

$$\mu=\phi^{+} \tag{2}$$

$$\sigma=(\partial\phi/\partial n_c)^{+} \tag{3}$$

where superscript $^{+}$ = a value at the limit of approaching P from the real-flow region.

Equations (1-3) define the relation between the strength of singularities on the boundary surface S and the induced potential at a point P. In a numerical simulation, the boundary surface is discretized to a panel assembly. The point P is called a "control point." A control point is different from a nodal point; thus, the position of the former may be decided independently from that of the latter unless the program scheme demands dependency.

In constructing Morino's scheme, there exist three methods of positioning the control point: 1) in the real-flow region (i.e., outside the panel assembly), 2) on the panel (using Cauchy's principal value integration), and 3) out of the real-flow region (i.e., inside the panel assembly). The algebraic equations for each case are obtained by discretizing Eq. (1), and become

$$\sum_{j=1}^{j\max}(\delta_{ij}-a_{ij})\mu_j-\sum_{k=1}^{k\max}b_{ik}\sigma_k=0$$

$$(i=1,2,\ldots,j\max) \tag{4}$$

for the first and the second methods and

$$\sum_{j=1}^{j\max}a_{ij}\mu_j+\sum_{k=1}^{k\max}b_{ik}\sigma_k=0$$

$$(i=1,2,\ldots,j\max) \tag{5}$$

for the final method. Here, i is a control-point index number, j and k are nodal-point index numbers for doublet and source, respectively, μ_j and σ_k are the doublet and source strength, respectively, on the nodal points, a_{ij} and b_{ik} are influence coefficients, and δ_{ij} is the Kronecker delta. For a linear distribution in the present work, each influence coefficient represents an influence of a nodal point via its adjacent panels (see Fig. 2). In the case of the first method, every control point must approach the nodal point of the same index number infinitely, i.e., $P_i \to Q_j$ where $j=i$, because Eq. (2) must be utilized to make the system of Eq. (4) closed. Similarly, each control point must be just on the nodal point in the case of the se-

cond method. The final method, however, imposes few restrictions on the positions of the control points except that they must be inside the panel assembly. This comes from the fact that the potential at each control point is zero, and that no other independent variables appear in the left-hand side of Eq. (5), even if the control point is positioned away from any nodal points. The arbitrariness of the control-point position removes the difficulties that appear in calculating influence coefficients when the control point is on the plane including the panel or on the straight line including the panel edge. This fact is also applicable to the VBC scheme in determining the positions of the inner control points.

Program Scheme

When Morino's scheme is applied, the panel assembly is formed to approximate the shape of the body and the wakes, and the distribution of source strength is determined explicitly with the mass flux boundary condition, i.e.,

$$\sigma_k = -\boldsymbol{U}\cdot\boldsymbol{n}_k \quad (k=1,2,\ldots,k\max) \tag{6}$$

where $\boldsymbol{n}_k$ is a unit normal to the panel assembly on the kth nodal point for source and $\boldsymbol{U}$ is the freestream velocity vector. The component of freestream velocity normal to the panel surface is approximately cancelled by this condition. The doublet strength on each nodal point is determined so that the perturbation velocity potential vanishes at any points inside the panel assembly. For this purpose, control points are distributed inside the domain of the panel assembly. The total number of control points is equal to that of the nodal points on the body panels. The positions of the control points can be chosen practically arbitrarily as shown before, which simplifies the evaluation of influence coefficients. The strength of the doublet is determined by setting the potential on the control points to zero, i.e., by solving Eq. (5).

In the velocity boundary condition (VBC) scheme, not only the doublet strength but also the source strength must be determined implicitly in order to ensure strict tangency. "Outer control points" are distributed on the body surface, and the flow is set to be tangent to the surface at those points, i.e.,

$$\sum_{j=1}^{j\max}(\boldsymbol{a}_{i'j}\cdot\boldsymbol{n}_{i'})\mu_j + \sum_{k=1}^{k\max}(\boldsymbol{b}_{i'k}\cdot\boldsymbol{n}_{i'})\sigma_k + \boldsymbol{U}\cdot\boldsymbol{n}_{i'} = 0 \quad (i'=1,2,\ldots,k\max) \tag{7}$$

where i' is an outer control-point index number, $\boldsymbol{n}_{i'}$ is a unit normal to the body surface on the control point, and $\boldsymbol{a}_{i'j}$ and $\boldsymbol{b}_{i'k}$ are velocity influence coefficient vectors. Additional conditions represented by Eq. (5) must be imposed on the "inner control points" in the same manner as in Morino's scheme (see Fig. 3). The unknowns μ_j and σ_k are obtained by solving Eqs. (5) and (7) simultaneously. It should be noted that the velocity boundary condition is imposed on the outer control points but not on the nodal points or on the panels. Thus, the panel assembly need not approximate the body shape in this scheme, because the former can be positioned apart from the outer control points.

Since the potential at a control point is not influenced by its downstream region in a supersonic flow, wakes are not needed in some types of flows, e.g., a flow around a wing with a supersonic trailing edge. However, there is a need for wakes for other types of flows: a flow around a wing with a subsonic trailing edge, around a wing-body shape, etc. In these cases, wakes are shed from the trailing edges of the wings. For a wing-body shape, the wake is linked to the body. Each wake consists of two panel assemblies overlaid, each of which is considered as the extended part of the upper and the lower surface of the wing, respectively. On the assemblies, there are distributed rows of nodal points of doublet, each of which is placed on the common vertex of its adjacent panels, and every row is connected with a nodal point on the trailing edge (see Fig. 4). Here, two nodal points exist at the same point on the trailing edge, one belonging to the upper surface and the other to the lower. Doublets alone are distributed on the wake panels. The influence of nodal points on the wake is added to the respective influence coefficients of their connected trailing-edge nodal points, because the doublet strength can be set constant on each row.[5]

Pressure coefficients on each panel are evaluated from the strengths of doublet on the vertices of the panel in the cases of Morino's scheme. In the cases of the VBC scheme, the coefficients on each outer control point are given from the solutions and velocity influence coefficients.

Results

Morino's scheme is employed in most cases. Thus, it is not overtly mentioned in this section when the method is restricted to this scheme.

Flows around Cones

An example of the panel assemblies used in the simulations of flows around cones is shown in Fig. 5. Pressure distributions on the panel surface obtained in the cases of

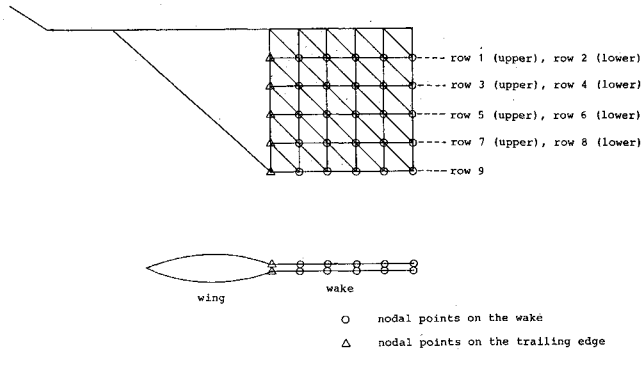

Fig. 4 Rows of nodal points on the wake panels.

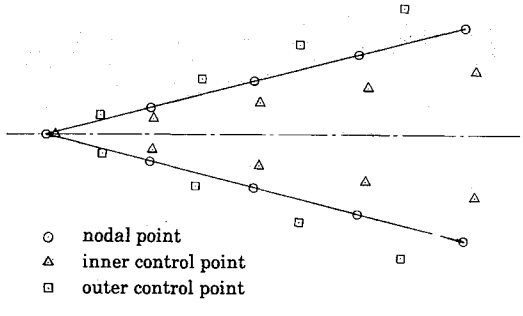

Fig. 3 Outer and inner control points.

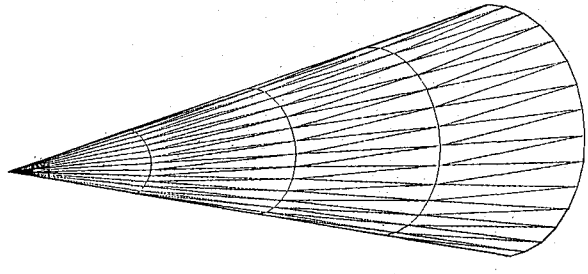

Fig. 5 A panel assembly simulating a cone.

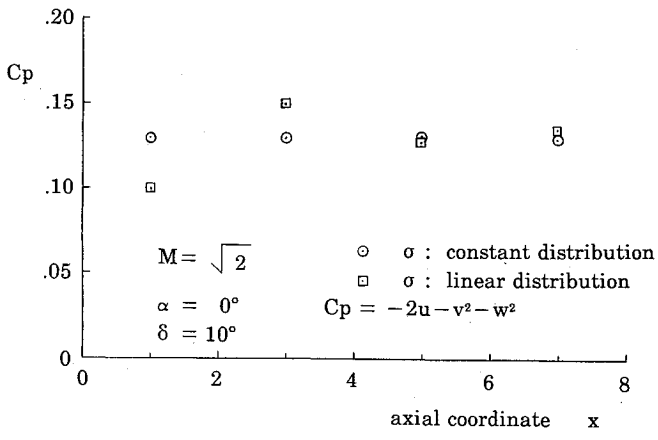

Fig. 6 Pressure distributions on a cone.

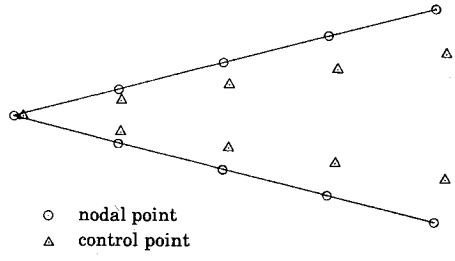

Fig. 7 An example of the distributions of nodal and control points.

constant and linearly varying sources are compared in Fig. 6. The doublet distribution is kept linear in both cases; the cone half-angle $\delta = 10$ deg, the angle of attack $\alpha = 0$ deg, and the freestream Mach number $M = \sqrt{2}$. In the case of a linear source distribution, the source strength σ at the cone tip is set at zero. The result of the constant source shows better agreement with theoretically predicted constant pressure than that of the linear source; thus, constant source distributions are used in the following simulations.

To prove the arbitrariness of control-point positions, their distributions are varied in three ways and compared. Each control point is shifted from the position of the nodal point of the same index number by distance d to the direction opposite to the outer normal of body surface (see Fig. 7). This method of control-point determination is adopted to prevent the diagonal elements of the doublet influence-coefficient matrix from being zero, thus avoiding the singularity of the algebraic equations. Such care is not needed in subsonic or incompressible flows. The length d is set as follows:

for case 1: $d = 0.005 l_1$
for case 2: $d = 0.005 l_1$ (at the cone tip)
$d = 0.2r$ (other than tip)
for case 3: $d = 0.005 l_1$ (at the cone tip)
$d = 0.5r$ (other than tip)

where l_1 = length of the downstream side edge of the upmost stream panel and r = cone radius at the respective position.

As shown in Table 1, the results of cases 1 and 2 coincide almost exactly, though the influence coefficients themselves are very different from each other. This proves that the control points can be displaced from the nodal-point positions or the panels. In case 3, however, the pressure coefficients diverge on the panel of the downstream region. It is found that the influence-coefficient matrix becomes less diagonally dominant as distance d increases, and the divergence in the third case is caused by the computational round-off error in the matrix inversion. This prohibits each control point from separating excessively far from the nodal point of the same index number. But this limitation does not reduce the advantage of the arbitrariness of the control-point positions in calculating the influence coefficients. In the following simulations, however, the distances between control points and nodal points are set to be no more than 10^{-3} times the representative length of the configurations, which was found to be enough to avoid difficulty in calculating the influence coefficients. It should be noted again that displacing control points from nodal points causes no mathematical error, as was proved by the preceding simulations. Computational round-off error is caused by the other mechanism. It was found in the procedure of the following simulations that the distances previously cited are small enough to prevent this kind of error from having harmful effects on the numerical procedures for various configurations having vastly different length scales and closely coupled surfaces of different panel spacings.

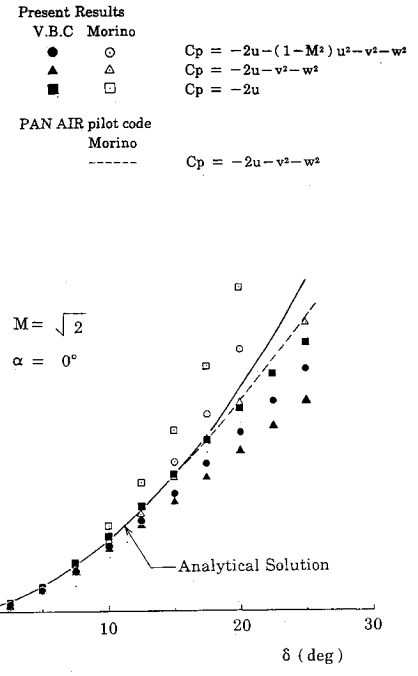

Fig. 8 Pressure coefficients vs cone half-angle.

Table 1 Pressure distributions on a cone

x	1.3	3.0	5.0	7.0
Case 1	0.1350	0.1349	0.1349	0.1349
Case 2	0.1350	0.1350	0.1350	0.1350
Case 3	0.1350	0.1350	Diverge	Diverge

$Cp = -2u - (1 - M^2)u^2 - v^2 - w^2$. x = axial coordinate.

Results of varying two parameters δ and M by keeping $\alpha = 0$ deg are shown in Figs. 8 and 9. Pressure distributions around a cone are shown in Fig. 10, where the parameters are set to $\alpha = 5$ deg, $\delta = 10$ deg, and $M = 1.5$. Both Morino's scheme and the VBC scheme are employed. Pressure coefficients are evaluated using three kinds of approximate expressions. In every figure, analytical solutions[7-10] and the results of the PAN AIR pilot code[3] are also shown. It cannot be predicted theoretically which expression for the pressure coefficient yields the best results, for the fundamental equation has already been linearized. The differences between their results, however, can be an indication of the perturbation's magnitude relative to the freestream velocity and can thus show a criterion of the correctness of the linearization in each case.

It can be concluded from the figures that the present results agree satisfactorily with analytical solutions, especially for the

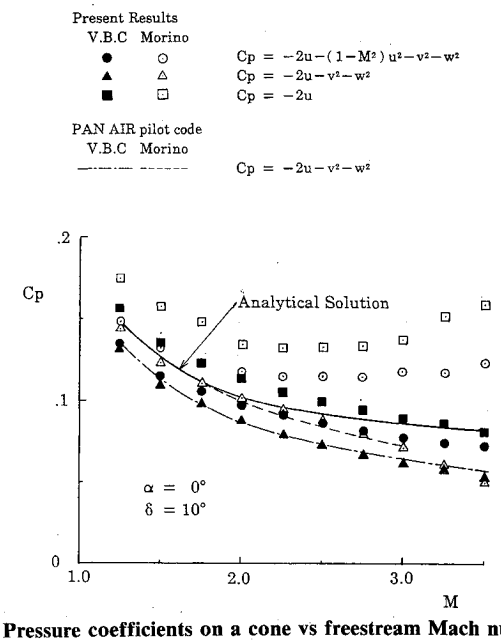

Fig. 9 Pressure coefficients on a cone vs freestream Mach number.

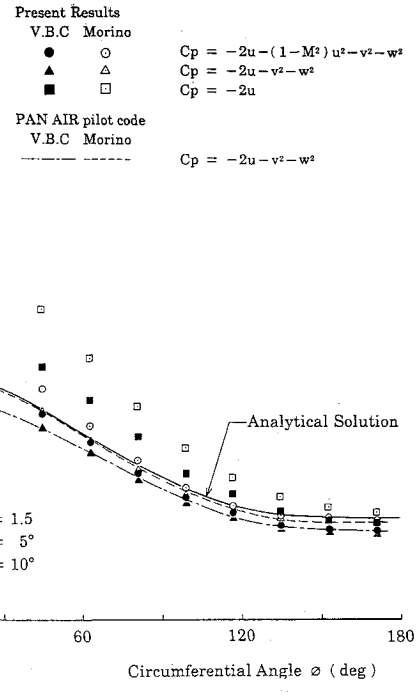

Fig. 10 Pressure distribution around a cone.

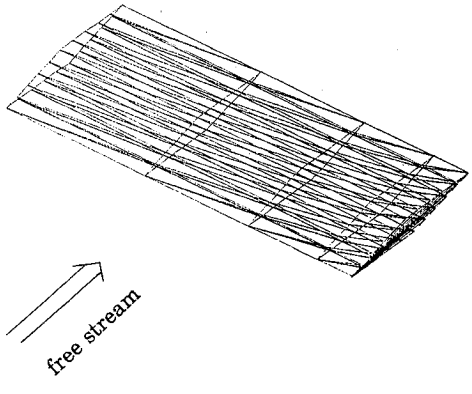

Fig. 11 A panel assembly simulating a double-wedge wing.

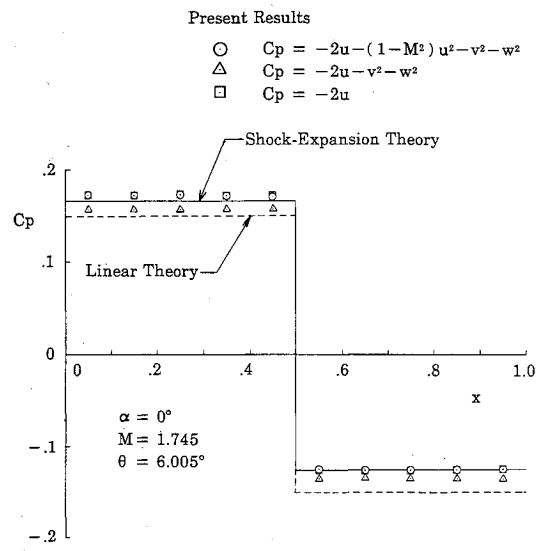

Fig. 12 Pressure distribution on a double-wedge wing.

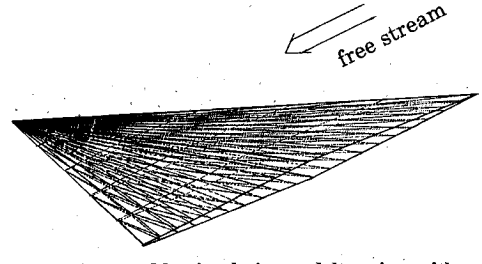

Fig. 13 A panel assembly simulating a delta wing with a diamond section.

VBC scheme, unless the perturbation is too large. However, the differences caused by the variation of pressure coefficient expressions are increased in the results of Morino's scheme compared with those in the VBC scheme's results. Deviations from analytical solutions are also increased in Morino's scheme in most cases. These are believed to be caused by the penetrating flow through the panel surface, which cannot be prohibited perfectly by the mass flux boundary condition employed in Morino's scheme. The trend of the present results is the same as that of the PAN AIR pilot code,[3] although the conclusions are partially different, for the results of the latter are restricted in the cases of the expression $Cp = -2u - v^2 \doteq w^2$, and the results of the VBC scheme are omitted in their figure corresponding to Fig. 8 in this paper. This suggests that equivalent computations can be performed by both programs, though the scheme of the present one is much simpler than that of the PAN AIR pilot code.

Flows around a Double-Wedge Wing

Half of the total panel assembly simulating a double-wedge wing is shown in Fig. 11. The flow is kept two-dimensional except in the wing tip region, and the chordwise pressure distribution can be obtained easily by the shock-expansion theory or the linear theory, both of which are shown in Fig. 12 for the case of $M = 1.745$ and $\alpha = 0$ deg. They are compared with the present computational result using three types of expressions for pressure coefficients. The latter agrees well with the former two.

Flows around a Delta Wing

A half-model of a delta wing with a diamond section used in the computation is shown in Fig. 13. Here, the sweep angle of the leading edge is 45 deg and the thickness ratio is 0.05. Chordwise pressure distributions obtained by the present simulation and by an analytical method[11] are shown in Figs. 14a-c by setting $\alpha = 0$ and 1 deg, and $M = 2.0$. The

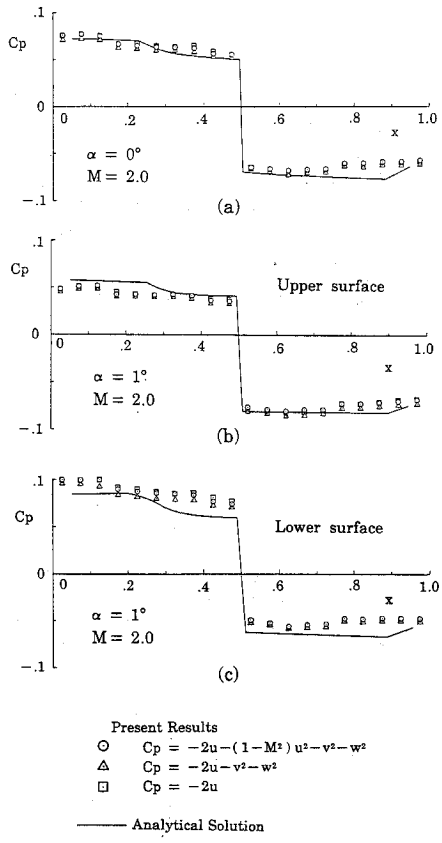

Fig. 14 Chordwise pressure distribution on a delta wing with a diamond section.

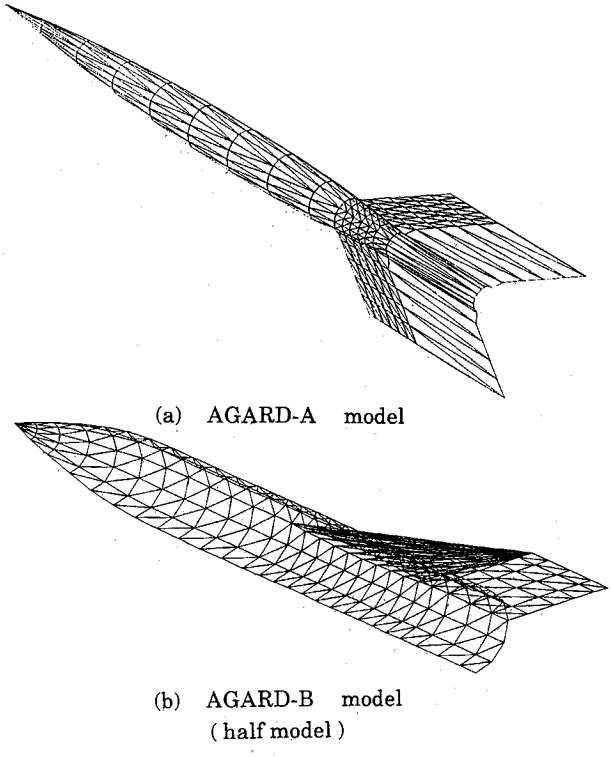

Fig. 15 Panel assemblies simulating wing-body configurations.

spanwise coordinate y is set 0.25 times half-span in the analytical solutions, but in the present results, it extends to the width of the panels. However, the agreement is almost right except for the positions where the influence of the wing's vertex or of the ridge lines' intersecting point appears. This can be caused by extension of the panels.

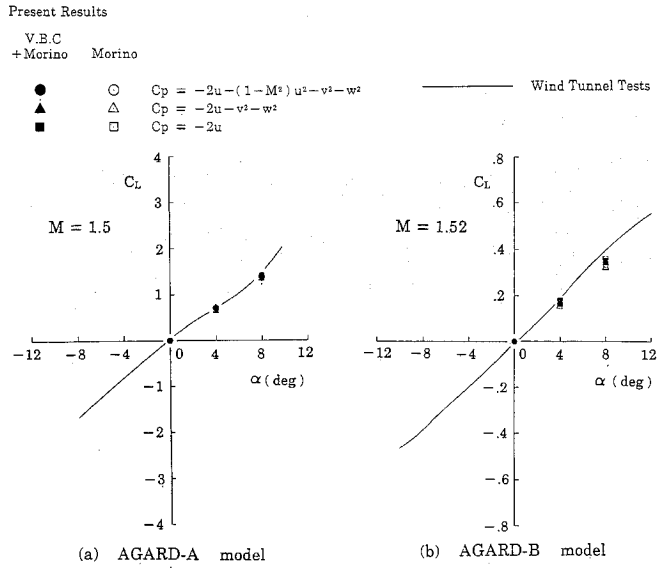

Fig. 16 Lift coefficients vs angle of attack.

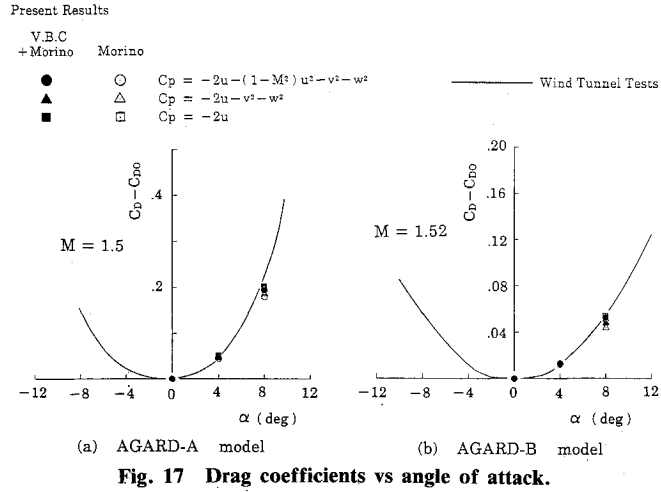

Fig. 17 Drag coefficients vs angle of attack.

Table 2 Examples of CPU time

Configuration	Total number of panels[a]	Total number of nodal points[a]	CPU time (s)
Double-wedge wing	180	106	60
Delta wing	360	206	171
AGARD-A	404	230	300
AGARD-B	578	329	514

[a]The number of panels or nodal points contained in the half model.

Flows around Wing-Body Configurations

The panel assemblies used in the simulations of flows around wing-body configurations (AGARD-A and -B models) are shown in Fig. 15. The wake of the AGARD-A's body is treated as a part of the body in the main procedure, but the aerodynamic force on it is not counted in the calculation of total force. Morino's scheme is employed in the simulations of flows around the entire configurations, and the VBC scheme is also utilized to simulate the flows around the forebodies, where the perturbation's magnitude may be considerably larger. Total force is calculated by integrating the pressure on each panel. Here, the pressure distribution is obtained from Morino's scheme alone or is partially replaced by that given by the VBC scheme. The numerical results for lift and drag coefficients for the cases of $\alpha = 0$, 4, and 8 deg are shown in Figs. 16 and 17, respectively, together with the results of wind tunnel tests.[12,13] The experimental results are shifted so as to pass through the origin in Fig. 16, and the

zero-lift drag coefficients are subtracted from both results in Fig. 17. Numerical results for lift coefficients in the AGARD-A case coincide with those of the experiments almost exactly. Moreover, there is little dependence on the expression of pressure coefficients. In the AGARD-B case, however, the numerical results for C_L differ slightly from those of the experiments in the case of $\alpha = 8$ deg, and the fluctuation caused by the variation of pressure expressions is somewhat enlarged. The fluctuation is reduced by employing the VBC scheme at the forebody, and thus, it is considered to have some relation to the penetrating flow at the forebody region occurring in Morino's scheme. The consistency of $(C_D - C_{D0})$ between the simulations and the experiments is good in every case. If Morino's scheme is employed for the entire configurations, however, the fluctuations caused by the variation of pressure expressions are enlarged when $\alpha = 8$ deg in the case of both models.

Computation Time and Program Size

The examples of CPU time needed in the present simulations using Morino's scheme are shown in Table 2. The employed computer is IBM 4361-5. The time is within a reasonable limit, though the present program is a prototype, and techniques like far-field expansions, panel blocking, etc., are not utilized to reduce the computation time. This is enough to show the practicability of this program.

The program consists of three parts: preprogram, main program, and postprogram. The preprogram provides the data inherent in each configuration, and the postprogram evaluates the required data from the solutions obtained by the main program. The principal scheme is wholly included in the main program, which consists of a procedure of about 900 steps written in FORTRAN for version 1 and a procedure of about 1800 steps for version 2. Here, version 2 utilizes temporary data sets outside the CPU, while version 1 does not, and both versions employ Morino's scheme. The program size is comparable to those of the panel methods for incompressible or subsonic flow.

Conclusions

Supersonic flows about several types of configurations are simulated using a new panel-method program MARCAP. In constructing the program, clear definitions of a nodal point and a control point have made the scheme much simpler than the conventional ones. Triangular panels are used to provide contiguity of surface along panel edges. Morino's scheme is employed for most cases, and the velocity boundary condition scheme is also applied to some cases. The results for flows around cones, a double-wedge wing, a delta wing, and wing-body configurations show good agreement with analytical solutions or wind-tunnel tests unless the perturbation is too large to satisfy the assumption of linearized flow. The disagreements appearing in the large perturbation cases are reduced when the velocity boundary condition scheme is employed instead of Morino's scheme. The trend of the present results for flows around cones is the same as that of the PAN AIR pilot code, which suggests that equivalent computations can be performed by both programs, although the scheme of the MARCAP is much simpler than that of the PAN AIR pilot code. The present program is a prototype, but the computation time is within a reasonable limit. The program size is comparable to that of the panel method for incompressible or subsonic flow.

References

[1]Akishita, S., Kurosaki, R., Okada, K., and Hirata, T., "Theoretical Prediction of Roll Moment on Wing-Controlled Missiles," *Journal of Aircraft,* Vol. 23, Nov. 1986, pp. 808–813.

[2]Woodward, F.A., "Analysis and Design of Wing-Body Combinations at Subsonic and Supersonic Speeds," *Journal of Aircraft,* Vol. 5, Nov.–Dec. 1968, pp. 528–534.

[3]Ehlers, F.E., Epton, M.A., Johnson, F.T., Magnus, A.E., and Rubbert, P.E., "A Higher Order Panel Method for Linearized Supersonic Flow," NASA CR-3062, 1978.

[4]Carmichael, R.L. and Erickson, L.L., "PAN AIR–A Higher Order Panel Method for Predicting Subsonic or Supersonic Linear Potential Flows About Arbitrary Configurations," AIAA Paper 81-1255, June 1981.

[5]Morino, L., Chen, L.T., and Suiciu, E.O., "Steady and Oscillatory Subsonic and Supersonic Aerodynamics around Complex Configurations," *AIAA Journal,* Vol. 13, March 1975, pp. 368–374.

[6]Ward, G.N., "The General Solutions of the Linearized Equations for Supersonic Flow," *Linearized Theory of Steady High-Speed Flow,* Cambridge University Press, Cambridge, England, 1955, pp. 45–64.

[7]Kopal, Z., "Tables of Supersonic Flow Around Cones," M.I.T., TR 1, 1947.

[8]Kopal, Z., "Tables of Supersonic Flow Over Yawing Cones," M.I.T., TR 3, 1949.

[9]Kopal, Z., "Tables of Supersonic Flow Around Cones of Large Yaw," M.I.T., TR 5, 1949.

[10]Roberts, R.C. and Riley, J.D., "A Guide to the Use of the M.I.T. Cone Tables," *Journal of the Aeronautical Sciences,* Vol. 21, May 1954, pp. 336–342.

[11]Jones, R.T. and Cohen, D., *High Speed Wing Theory,* Princeton University Press, Princeton, NJ, 1960.

[12]Takagi, K., Saito, H., and Ishihara, K., "Measurements of Aerodynamic Force of Supersonic Flow About AGARD-A Standard Model," (in Japanese), TM-38, National Aerospace Laboratory, Tokyo, Japan, June 1964.

[13]Takagi, K., Tani, T., Saito, H., and Arai, T., "Measurements of Aerodynamic Force on AGARD-B Standard Model in a Blow-Down Type 1m×1m Supersonic Wind Tunnel, (in Japanese), TM-20, National Aerospace Laboratory, Tokyo, Japan, July 1963.